The Effectiveness of determining the Load-bearing Capacity of Piles based on the Results of Pile Dynamic Testing: The Case Study of Long An Province, Vietnam

Phu-Huan Vo Nguyen
Infrastructural Technique Department, Faculty of Civil Engineering, Ho Chi Minh City Open University, Vietnam
huan.vnp@ou.edu.vn

Trong Nghia-Nguyen
Faculty of Civil Engineering, Ho Chi Minh City Open University, Vietnam
nghia.nt@ou.edu.vn (corresponding author)

Received: 21 November 2023 | Revised: 4 December 2023 | Accepted: 12 December 2023

 DOI: https://doi.org/10.48084/etasr.6651

ABSTRACT

Determining the load-bearing capacity of piles currently relies on various field experimental methods, with static pile compression loading testing and dynamic pile testing through Pile Driving Analysis (PDA) being widely accepted as reliable practices. However, the application of PDA tests faces limitations, especially in construction projects with weak soil profile while the static pile load test usually requires high testing costs. Consequently, the conventional dynamic pile testing method, checking the resistance through a number of dynamic hammer blows, is commonly utilized. Despite its prevalence, there has been limited research on the traditional dynamic pile testing method. In light of this, the present study aims to examine the traditional approach by analytical and numerical simulations. By doing so, it seeks to offer a more objective and comprehensive understanding of its effectiveness when compared to alternative methods.

Keywords-pile driving analysis; dynamic pile testing; pile bearing capacity; Plaxis software

I. INTRODUCTION

When evaluating the load-bearing capacity of piles, static pile compression loading testing emerges as the most reliable and extensively utilized method. This approach simulates the interaction between the pile and the surrounding soil, creating a critical state for the pile that encompasses ultimate skin friction and end bearing capacity. The testing procedure entails applying incremental loads and recording corresponding displacements. The ultimate bearing capacity of the pile becomes evident through the load-displacement graph constructed from these records. While notable advantages include its versatility and high reliability for various pile types, it is essential to acknowledge some significant drawbacks, such as the time-consuming nature of the testing process and the associated costs. However, assessing the load-bearing capacity of piles, especially for those with substantial lengths, inclined or submerged piles, the former presents challenges during static compression testing. The reliability of the results may be compromised in such scenarios. To address this, Pile Driving Analysis (PDA), a dynamic pile load test (PDA), capable of measuring large deformations, is employed to validate static pile compression test results [1]. Notably, the PDA technique offers the additional advantage of detecting the integrity of a pile. This detection is crucial in situations like pile driving where deflection or damage is common. Despite these advantages, PDA accuracy hinges on the technical proficiency of experimenters, given the complexity involved in assuming initial parameters for pile and soil profile, which can be used to construct a calculation model for dynamic analysis [2]. However, the PDA method results depend heavily on the specific soil conditions at the testing location. Soil heterogeneity can make the pile quality evaluation challenging. Moreover, the PDA equipment may require a significant initial investment, while conducting the tests also demands professionalism. This can contribute to an overall increase in project costs.

Evaluating the load-bearing capacity of piles through traditional pile dynamic analysis involves assessing the residual settlement of piles under dynamic loads, such as the number of blows required for a certain displacement. This method is relatively simple and cost-effective, making it suitable for a wide range of piles [3]. The experimental principle is rooted in Newton's laws, treating the pile as a rigid body with

concentrated soil resistance at the pile tip. Following a rest period for the soil beneath the pile tip to stabilize, a pile-driving hammer, either pneumatic or diesel, imparts an impact force to the pile head. The hammer energy corresponds to the total soil resistance, leading to pile settlement and energy loss during the driving process [7]. Despite its simplicity and cost-effectiveness, this method accuracy is not optimal, prompting the need for further research to refine and enhance its precision, with the goal of reducing experimental and project expenses.

In this paper, within a case study context of a construction project which includes port, embankments, hydraulic structures, and small to medium-sized bridges with pile foundations, the practical assessment of pile load-bearing capacity compared to design requirements often hinges on the dynamic pile testing outcomes. This method is crucial for determining the appropriate pile length for general construction purposes. Recognizing this approach significance, the research focuses on the traditional dynamic pile testing method, which predicts pile load-bearing capacity based on pile driving refusal. The aim is to strengthen the theoretical foundations, and validate the dependability of computational results, aligning with the prevalent practices in the Vietnamese construction landscape.

II. PROJECT INFORMATION

Project location: The Binh Dien Fertilizer Plant is situated on the left bank of the Vam Co Dong River, downstream from the Ben Luc Bridge, in Long Dinh Commune, Can Duoc District, Long An Province.

Project scale: 3000DWT wharf, on pile foundation consisting of 126 pre-stressed concrete piles D600-C, with pile lengths ranging from 34 m to 36 m.

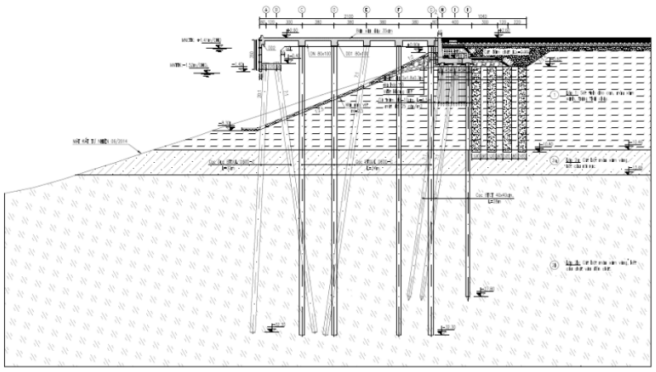

Fig. 1. Cross-sectiol of the structure.

D600-C is composed of pre-stressed concrete piles with the following specifications:

- Outer diameter: $d = 0.6$ m
- Wall thickness: $t = 0.1$ m
- Pile tip cross-sectional area: $A_b = 0.283$ m^2
- Circumference of the the pile: $u = 1.885$ m
- Concrete strength of the pile: R_b=60 MPa
- Elastic modulus: E_b=28.5×103 MPa
- Maximum axial load: 414 T
- Suitable construction load: 373 T
- Crack resistance moment: $M_{cr} \geq 29$ Tm

Details of the piles before conducting dynamic testing can be seen in Table I.

TABLE I. PILE ELEVATION OF 4 TESTED PILES (m)

No.	Pile top elevation	Pile tip elevation
Pile A3 – 34 m length	+1.32	-32.68
Pile D8 – 36 m length	+2.53	-33.47
Pile F12 – 36 m length	+3.65	-32.35
Pile C17 – 36 m length	+3.70	-32.30

III. PILE LOAD-BEARING ANALYSIS

A. Load-bearing Capacity of Ailes according to the Geotechnical Criteria of the Soil

Calculations were done according to Section 7, Vietnam Standard 10304:2014. The ultimate compressive load-bearing capacity *Rc,u* (kN) of a suspended or driven pile is determined by the sum of the resistance of the soil beneath the pile tip and along the pile shaft:

$$R_{c,u} = \gamma_c \left(\gamma_{cq} q_b A_b + u \sum \gamma_{cf} f_i l_i \right) \quad (1)$$

where γ_c is the working condition factor of the pile in the soil, q_b is the resistance strength of the soil beneath the pile tip, A_b is the area of the pile bearing on the soil, taken as the cross-sectional area of the pile tip, including the capped tip, u is the circumference of the cross-sectional area of the pile shaft, f_i is the average resistance strength of the i^{th} soil layer along the pile shaft, l_i is the length of the pile segment within the i^{th} soil layer, and γ_{cq} and γ_{cf} are the working condition factors of the soil beneath the pile tip and along the pile shaft, considering the influence of the pile driving method on the soil resistance.

The allowable compressive load-bearing capacity of piles, based on the soil geotechnical criteria, with γ_k being the reliability factor regarding the soil in the high-rise pier foundation case, is dependent on the number of piles in the foundation:

$$R_{c,d} = \frac{R_{c,u}}{\gamma_k} \quad (2)$$

The results of pile load-bearing from (2) are displayed In Table II.

TABLE II. PILE LOAD-BEARING CAPACITY OF 4 TESTED PILES ACCORDING TO THE GEOTECHNICAL CRITERIA OF THE SOIL (TON)

No.	$R_{c,u}$	$R_{c,d}$
Pile A3	278.95	199.25
Pile D8	289.01	206.44
Pile F12	274.79	196.28
Pile C17	274.16	195.83

B. Load-bearing Capacity of Piles according to Standard Penetration Test (SPT)

Calculations were done according to Appendix G, Vietnam Standard 10304:2014. The ultimate compressive load-bearing capacity Rc,u (kN) is:

$$R_{c,u} = q_b A_b + u\sum\left(f_{c,i}l_{c,i} + f_{s,i}l_{s,i}\right) \quad (3)$$

where q_b is the resistance strength of the soil beneath the pile tip, A_b is the area of the pile bearing on the soil, taken as the cross-sectional area of the pile tip, including the capped tip, u is the circumference of the cross-sectional area of the pile shaft, $f_{c,i}$ is the average resistance strength along the pile segment within the i^{th} cohesive soil layer, $l_{c,i}$ is the length of the pile segment within the i^{th} cohesive soil layer, $f_{s,i}$ is the average resistance strength along the pile segment within the i^{th} loose soil layer, and $l_{s,i}$ is the length of the pile segment within the i^{th} loose soil layer.

The allowable compressive load-bearing capacity of piles according to SPT, with FS being the Factor Safety (from 2.0 to 3.0) is:

$$R_{c,d} = \frac{R_{c,u}}{FS} \quad (4)$$

The results of pile load-bearing from (4) are displayed in Table III.

TABLE III. PILE LOAD-BEARING CAPACITY OF 4 TESTED PILES ACCORDING TO SPT (TON)

No.	$R_{c,u}$	$R_{c,d}$
Pile A3	408.64	136.21
Pile D8	486.64	162.21
Pile F12	418.72	139.57
Pile C17	406.92	135.64

C. Load-bearing Capacity of piles according to the PDA test

a) SMITH Model

The Smith model employs the finite difference method to find a solution to the stress wave equation under ultimate load. Smith model transforms the stress wave transmission equation into a system of discrete element differential equations in the pile-soil-hammer system [8].

b) CASE Model

The Case model employs the principle of stress wave transmission in a one-dimensional rod, measuring the force and particle velocity waves at the pile head. The model analyzes the wave graphs to determine the pile load-bearing capacity [9]. The Case model allows for the calculation of load-bearing capacity to be performed immediately after the experiment concludes. The calculation method does not rely on the matching of assumed calculated signal waves and measured real waves, which distinguishes it from the other two models.

c) CAPWAP Model

The CAPWAP (Case Pile Wave Analysis Program) model is also known as the signal matching method. The CAPWAP model inherits and combines the Smith and Case models based on the common principle of stress wave transmission. On this basis, the CAPWAP model constructs both the pile model and the soil model [10, 11]. The CAPWAP model is an improved and more advanced version of the Smith model. It considers additional behaviors in the pile-soil system that the Smith model does not address. Some of them are: the propagation of dynamic resistance, the unloading and reloading process, the dynamic resistance of pile materials, the behavior of pile tips on stiff ground, and the elastic-visco-plastic behavior of the soil.

The results of the pile load-bearing from PDA test by the CAPWAP model are shown in Table IV.

TABLE IV. PILE LOAD-BEARING OF 4 TESTED PILES ACCORDING TO THE PDA TEST (TON)

No.	$R_{c,u}$	$R_{c,d}$
Pile A3	265.0	189.29
Pile D8	271.2	193.71
Pile F12	266.3	190.21
Pile C17	285.5	203.93

D. Load-bearing Capacity of Piles according to Dynamic Pile Testing

The experiment is based on Newton's laws with the assumption that the pile is a rigid body and the soil resistance is concentrated at the pile tip. After a resting period, allowing the soil beneath the pile tip to return to a stable state, a pile-driving hammer is used to apply an impact force to the pile head [12, 13]. The energy of the pile-driving hammer is equal to the soil total resistance, resulting in pile residual settlement and energy loss during pile driving. The anticipated dynamic pile residual settlement calculated according to Vietnam Standard 9394:2012 is:

$$e \le \frac{nFE_{tt}}{\frac{kP}{M}\left(\frac{kP}{M}+nF\right)} \times \frac{Q_T + \varepsilon^2(q+q_1)}{Q_T + q + q_1} \quad (5)$$

where e is the residual settlement, equal to the pile settlement due to one blow of the pile-driving hammer (m), k is the soil safety factor, depending on the number of piles in the foundation, P is the calculated load-bearing capacity of the pile (T), E_{tt} is the calculated energy of one hammer blow (T.m), Q_T is the total weight of the hammer (T), q is the weight of the pile and pile cap (T), q_1 is the weight of the pile cushion (T), M is a factor equal to 1.0 for pile driving, n is a factor equal to 150 for precast concrete piles with caps (T/m²), ε^2 is the rebound restitution coefficient, taken as 0.2 when driving precast concrete piles with caps ,and F is the cross-sectional area of the pile according to the outer perimeter (m²).

The results of pile load-bearing from the Dynamic Pile Testing are shown in Table V.

TABLE V. PILE LOAD-BEARING CAPACITY OF 4 TESTED PILES ACCORDING TO THE PDA TEST (TON)

No.	$R_{c,u}$	$R_{c,d}$
Pile A3	170.40	121.71
Pile D8	194.16	138.68
Pile F12	185.40	132.43
Pile C17	273.94	195.67

E. Load-bearing Capacity of Piles according to the Finite Element Method (Plaxis software)

1) Subsoil Model

The Mohr–Coulomb model approximately simulates the stress–strain relationship of the soil based on the elastic–plastic law [4]. The Hardening Soil model simulates the stress–strain relationship of the soil using a Hyperbolic curve reached from the elastoplastic theory instead of the elastic theory. Therefore, the Hardening Soil model has the capability to simulate non-reversible stress–strain behavior, making it more accurate in representing the real soil characteristics [5, 6]. Three elastic moduli, E^{ref}_{50}, E^{ref}_{oed}, E^{ref}_{ur}, were selected based on the results of triaxial CU tests and unconfined compression tests on all soil layers investigated in this study.

2) Input Data in Plaxis

The considered parameters used as input in Plaxis can be seen in Tables VI and VII.

TABLE VI. SOIL PARAMETERS IN PLAXIS

	Unit	Layer 1	Layer 2A	Layer 2B (above)	Layer 2B (below)
Type		HS	HS	HS	HS
γ_{unsat}	kN/m^3	15.2	20.4	20.5	20.5
γ_{sat}	kN/m^3	15.46	20.82	20.89	20.89
E^{ref}_{50}	kN/m^2	2700	10000	15000	23000
E^{ref}_{oed}	kN/m^2	2700	10000	15000	23000
E^{ref}_{ur}	kN/m^2	8100	30000	45000	69000
m		0.7	0.6	0.6	0.5
ν_{ur}		0.34	0.3	0.25	0.25
c	kN/m^2	12.9	14.4	14	14
φ	(o)	12.15	24.7	25.7	25.7
ψ	(o)	0	0	0	0
R_{inter}		0.6	0.7	0.8	0.8

TABLE VII. PILE PARAMETERS IN PLAXIS

Pile D600-C	Symbol	Unit	Value
Type			Elastic
Mass per meter length of the pile	w	kN/m/m	4.08
Mass moment of inertia	I	m^4	0.00511
Elastic modulus	E	KN/m^2	2.85E+07
Poisson's ratio	ν		0.2
Compression stiffness	E.A	KN/m	4.477E+06
Flexural stiffness	E.I	KN/m^2/m	1.455E+05

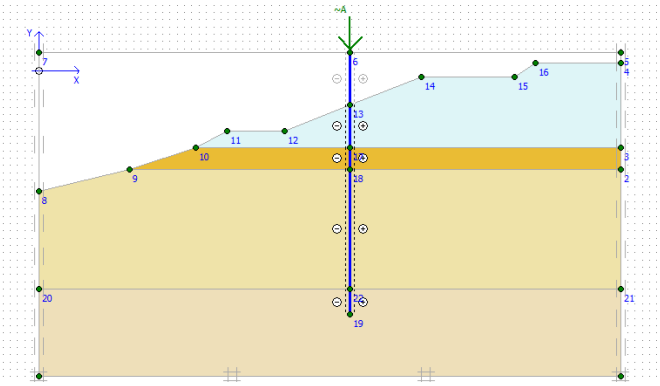

Fig. 2. Cross-section of the structure in Plaxis.

3) Calculation Model

The geometry and the calculation model of the project are shown in Figure 2.

4) Modeling Calculation Results

Figure 3 illustrates the plot of the vertical displacement of the pile head over time (Dynamic time - *Uy*). The results of the pile displacement (deflection), as the oscillation gradually diminishes until stability is reached, can be observed.

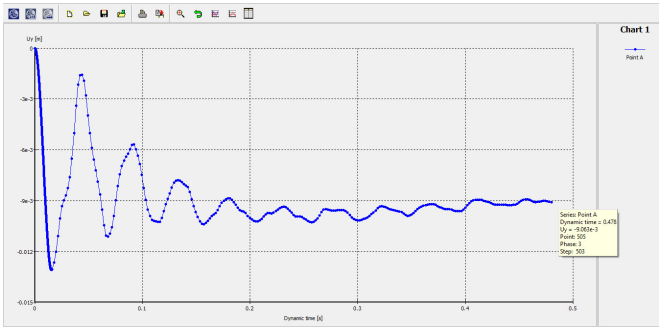

Fig. 3. Graph of vertical displacement at the head of pile D8 (*Uy*) over time.

The output outcomes of the maximum axial force appearing in the pile is the sum of the reactions from the soil below the pile tip acting on the pile and the friction along the perimeter of the pile that is mobilized to the maximum during the pile subjection to dynamic loading. The results from the envelope of bending moment diagram contribute to structural design optimization, allowing for adjustments in materials, dimensions, or other parameters to meet the specific criteria (Figure 4).

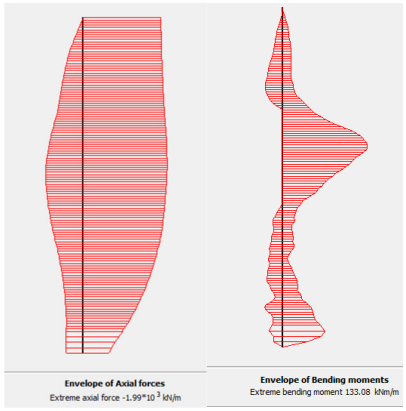

Fig. 4. Axial forces and bending moments at pile D8.

TABLE VIII. PILE LOAD-BEARING CAPASITY OF 4 TESTED PILES ACCORDING TO MODELING (TON)

No.	$R_{c,u}$	$R_{c,d}$
Pile A3	197	140.71
Pile D8	199	142.14
Pile F12	201	143.57
Pile C17	199	142.14

IV. PILE LOAD-BEARING COMPARISON

In this segment, the comparison of the ultimate bearing capacity and the allowable load-bearing capacity of the piles among various approaches is illustrated in Figures 5 and 6.

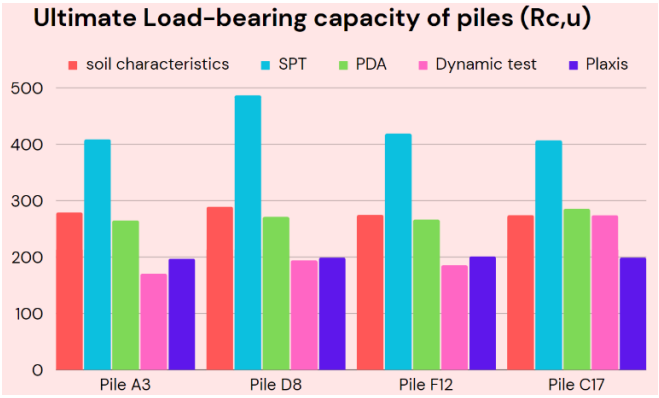

Fig. 5. Comparison of pile ultimate bearing capacity results.

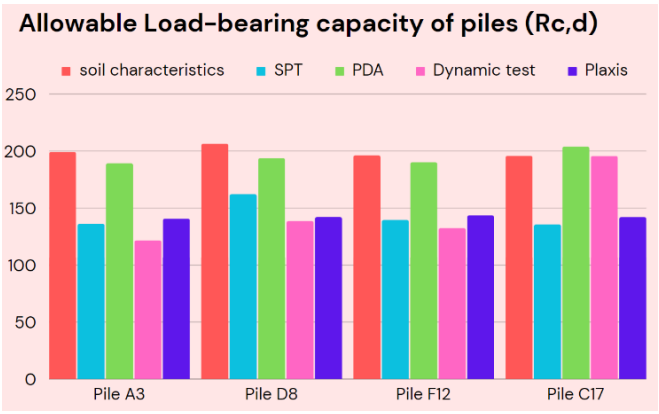

Fig. 6. Comparison of allowable pile load-bearing capacity results.

Figure 5 reveals that the ultimate bearing capacity, which is predicted based on the SPT values, consistently yields notably higher values, than the other methods, with the difference reaching 100 tons. However, Figure 6 indicates less variability in the allowable load across the techniques, with a maximum difference of approximately 50 tons. This discrepancy may be attributed to the factor of safety applied in accordance with Vietnamese standards. Engineers should exercise caution when employing each method for bearing capacity determination within the context of these standards. The traditional dynamic approach consistently shows lower ultimate bearing capacity values from the other techniques, as depicted in Figure 5. Notably, in the case of pile C17, the dynamic approach records a higher bearing capacity of 273.94 tons compared to an average of around 200 tons for piles A3, D8, and F12. Interestingly, the results from numerical simulation with Plaxis align with the traditional dynamic approach outcomes. Figures 5 and 6 also highlight a noteworthy agreement between the bearing capacity as determined by soil characteristics and PDA. The consistent values suggest that PDA serves as a reliable method for foreseeing pile responses. Particularly, the allowable load in Figure 6 demonstrates that the two techniques, utilizing soil characteristics and PDA, yield higher values than the other approaches.

V. CONCLUSION

This study undertook a thorough investigation into the bearing capacity and allowable loading of piles, utilizing five distinct approaches, with a particular emphasis on the economical and time-efficient traditional dynamic approach. The key findings and implications of this study are:

- Traditional Dynamic Approach Reliability: The results of ultimate bearing capacity and allowable load obtained through the traditional dynamic approach exhibit agreement with the numerical simulation in Plaxis, highlighting its reliability. However, variations, notably in the case of pile C17, indicate certain limitations that engineers should consider in practical applications.
- PDA and Soil Characteristics: The consistently demonstrated validity of the results from PDS and soil characteristic approaches establishes PDA as a reliable method for determining pile responses. Additionally, the allowable load predictions from these approaches consistently surpass those of the other methods.
- SPT Approach Considerations: While the bearing capacity predicted from the SPT approach exhibited the highest values, the allowable load predictions demonstrate smaller values, potentially influenced by the safety factor determined by Vietnamese standards. Caution is recommended in practical applications.
- Future Research Directions: To enhance the understanding of field-measured pile driving deflection in various structural scenarios, using pile foundation methods, extensive research is recommended. Future work should encompass diverse geological and subsurface conditions, including medium sand, coarse sand, stiff clay, semi-stiff clay, among others. Such investigations will contribute to refining and advancing current practices in the field.

REFERENCES

[1] P. Middendorp and C. Zandwijk, "Accuracy and Reliability od Dynamic Pile Testing Techniques," in *Proceedings of the 4th International Conference on Behaviour of Offshore Structures (Boss '85)*, The Netherlands, Jan. 1985.

[2] M. F. Randolph, "Analysis of the Dynamics of Pile Driving," in *Advanced Geotechnical Analyses*, CRC Press, 1991.

[3] G. Likins and F. Rausche, "Correlation of CAPWAP with Static Load Tests," in *Proceedings of the Seventh International Conference on the Application of Stresswave Theory to Piles*, Selangor, Malaysia, 2004, pp. 153–165.

[4] P. H. V. Nguyen and P. C. Nguyen, "Effects of Shaft Grouting on the Bearing Behavior of Barrette Piles: A Case Study in Ho Chi Minh City," *Engineering, Technology & Applied Science Research*, vol. 11, no. 5, pp. 7653–7657, Oct. 2021, https://doi.org/10.48084/etasr.4389.

[5] T.-D. Tran and P.-H. V. Nguyen, "Computation of Limit Loads for Bending Plates," *Engineering, Technology & Applied Science Research*, vol. 13, no. 2, pp. 10466–10470, Apr. 2023, https://doi.org/10.48084/etasr.5671.

[6] P. H. V. Nguyen, T. D. Tran, and P. C. Nguyen, "Effect Factors on Unconfined Compressive Strength of Soil-Cement Columns: The Case Study of Ba Ria, Vung Tau, Vietnam," *Engineering, Technology &*

Applied Science Research, vol. 13, no. 2, pp. 10352–10356, Apr. 2023, https://doi.org/10.48084/etasr.5681.

[7] F. Jia, Y. Tang, K. Hu, and Y. Wang, "Simulation Analysis on Pile-driving Process of Anti-flood Bionic Screw Pile," *IOP Conference Series: Materials Science and Engineering*, vol. 611, no. 1, Jul. 2019, Art. no. 012048, https://doi.org/10.1088/1757-899X/611/1/012048.

[8] A. Farshi Homayoun Rooz and A. Hamidi, "Numerical Analysis of Factors Affecting Ground Vibrations due to Continuous Impact Pile Driving," *International Journal of Geomechanics*, vol. 17, no. 12, Dec. 2017, Art. no. 04017107, https://doi.org/10.1061/(ASCE)GM.1943-5622.0001016.

[9] L. Gao, K. Wang, J. Wu, S. Xiao, and N. Wang, "Analytical solution for the dynamic response of a pile with a variable-section interface in low-strain integrity testing," *Journal of Sound and Vibration*, vol. 395, pp. 328–340, May 2017, https://doi.org/10.1016/j.jsv.2017.02.037.

[10] J. C. Cleary and E. J. Steward, "Analysis of ground vibrations induced by pile driving and a comparison of vibration prediction methods," *DFI Journal - The Journal of the Deep Foundations Institute*, vol. 10, no. 3, pp. 125–134, Nov. 2016, https://doi.org/10.1080/19375247.2017.1288855.

[11] K. C. Kuei, J. T. DeJong, and M. Ghafghazi, "Prediction, Performance, and Uncertainty in Dynamic Pile Load Testing as Informed by Direct Measurements from an Instrumented Becker Penetration Test," *Journal of Geotechnical and Geoenvironmental Engineering*, vol. 146, no. 8, p. 04020067, Aug. 2020, https://doi.org/10.1061/(ASCE)GT.1943-5606.0002290.

[12] A. Hamidi and A. Farshi Homayoun Rooz, "Efficiency analysis of open trench for impact pile driving through a single-variable method," *Marine Georesources & Geotechnology*, vol. 39, no. 1, pp. 82–102, Jan. 2021, https://doi.org/10.1080/1064119X.2019.1678706.

[13] J. Wu, K. Wang, and M. H. El Naggar, "Dynamic response of a defect pile in layered soil subjected to longitudinal vibration in parallel seismic integrity testing," *Soil Dynamics and Earthquake Engineering*, vol. 121, pp. 168–178, Jun. 2019, https://doi.org/10.1016/j.soildyn.2019.03.010.